Characterization and Efficacy of Titanium Dioxide Nano-Formulation on Skin Microflora Reduction and Wound Healing in Animals

Noppason Pangprasit , Yada Thammawong , Alongkorn Kulsirorat , Phongsakorn Chuammitri , Aphisek Kongkaew , Montira Intanon , Witaya Suriyasathaporn , Surachai Pikulkaew , Wasana Chaisri *

Posted Date: 11 July 2023

doi: 10.20944/preprints202307.0626.v1

Keywords: Animal wound; Anti-biofilm forming; Antimicrobial activities; Skin microflora; Titanium dioxide

Article

Characterization and Efficacy of Titanium Dioxide Nano-Formulation on Skin Microflora Reduction and Wound Healing in Animals

Noppason Pangprasit [1,2], Yada Thammawong [2], Alongkorn Kulsirorat [2], Phongsakorn Chuammitri [3,4], Aphisek Kongkaew [5], Montira Intanon [3,4], Witaya Suriyasathaporn [2,4], Surachai Pikulkaew [2,4] and Wasana Chaisri [2,4]

1 Akkhraratchakumari Veterinary College, Walailak University, Nakhon Si Thammarat 80160, Thailand
2 Department of Food Animal Clinic, Faculty of Veterinary Medicine, Chiang Mai University, Chiang Mai 50100, Thailand
3 Department of Veterinary Bioscience and Veterinary Public Health, Faculty of Veterinary Medicine, Chiang Mai University, Chiang Mai 50100, Thailand
4 Research Center of Producing and Development of Products and Innovations for Animal Health, Chiang Mai University, Chiang Mai 50100, Thailand
5 Research Administration Section, Faculty of Medicine, Chiang Mai University, Chiang Mai 50200, Thailand
* Correspondence: wasana.ch@cmu.ac.th, Tel: +66-53948023

Simple Summary: In veterinary fields infected wounds are one of the leading causes of morbidity and mortality in animals. Due to the widespread use of antibiotics in wound treatment, multidrug-resistant bacterial strains have emerged in animals and interest in alternative antimicrobial treatments has focused on the use of metal oxide nanoparticles. In this study, we have addressed this challenge using the application of a solution-stabilized dispersion of titanium dioxide nanoparticles (TiO_2-NP). This product has been investigated for its unique properties of countering specific members of the skin microflora and its enhancement of the wound healing process. It has been shown that TiO_2-NP with 383.10 ± 23.05 nm and the zeta potential 19.27 ± 4.65 mV are able to inhibit bacterial growth and biofilm formation of reference members of the skin microflora, *Staphylococcus aureus* and *Escherichia coli*, and enhance cell migration and wound healing processes in-vitro and in-vivo. TiO_2-NP is a promising candidate for veterinary medical applications that can be used to improve the wound healing process.

Abstract: The use of metal oxide nanoparticles as an alternative antimicrobial agent has gained attention due to the increasing problem of antibiotic resistance. Understanding its properties and potential benefits can contribute to the development of more effective and sustainable treatments in veterinary medicine. The aim of this study was to characterize TiO_2-NP formulations and evaluate their antibacterial and wound healing abilities. The diameters and zeta potentials were determined using the Zetasizer in conjunction with dynamic light scattering. The agar-well diffusion method, time-kill kinetic assay and crystal violet assay were used to evaluate their antimicrobial activities. Wound healing assays were conducted both in-vitro and in-vivo. The study demonstrated that TiO_2-NP formulations exhibit significant antimicrobial properties against various bacterial strains such as *S. aureus* and *E. coli*. No measurable *E. coli* growth was observed within a 15-mins period following exposure to TiO_2-NP formulations. The TiO_2-NP formation can improve wound healing by enhancing cell migration and collagen formation in both in-vitro and in-vivo conditions. In summary, our study suggests that TiO_2-NP has the potential for use as an antimicrobial agent for animal wound treatment due to its ability to suppress bacterial growth and biofilm formation, as well as to enhance wound healing.

Keywords: animal wound; anti-biofilm forming; antimicrobial activities; skin microflora; Titanium dioxide

 doi:10.20944/preprints202307.0626.v1

1. Introduction

Bacterial infections in animal wounds are a major concern for the global animal healthcare industry. The wound-related issues arise as a result of an infection by an external pathogen or skin microbiota, resulting in necrosis or slough, and impaired healing, subsequently leading to chronic wounds. Aerobic or facultative bacterial pathogens such as *Staphylococcus aureus*, *Streptococcus pyogenes*, *Pseudomonas* spp., *Escherichia coli*, *Enterococci* spp. etc. are the most common causative organisms associated with infected wounds [1,2]. When the wound healing process does not proceed in an organized and timely manner resulting in a chronic wound developing [3,4]. This adds to the burden by necessitating extended wound care, reducing the quality of animal life and increasing medicinal expenses. Generally, broad spectrum antibiotics and antiseptics are frequently used in wound management due to their cost-effectiveness and efficacy [5,6]. In spite of the fact that the extensive use of broad-spectrum antibiotics is a major contributor to the emergence of resistant bacteria, they are still widely used in the treatment of wounds. This has led to the emergence of multidrug-resistant bacteria on wound sites [7,8]. Furthermore, they are regarded as reservoirs for the transmission of antimicrobial resistance (AMR) to humans through close contact [9,10]. The spread of antimicrobial resistant bacteria is not the only aspect of the problem of antibiotic resistance. Biofilm formation is another bacterial strategy that contributes to their capacity to cause antibiotic resistance or tolerance. Biofilms, which are formed of extracellular polymeric substances that act as a protective layer, have become a major concern resulting in chronic wounds, an increase in multidrug-resistant bacterial strains, and a reduction in treatment efficiency [11]. The antibiofilm properties of various metal oxide with nanoparticles as well as their effect on plankton bacteria cells and biofilms [12], including ZnO (500 μg/ml) and TiO_2 (100 μg/ml) nanoparticles have been demonstrated against strong and weak biofilm-producing methicillin-resistant *Staphylococcus aureus* (MRSA) isolates [13].

For this reason, nanotechnology is a recognized and reliable research field for improving the efficacy of treatment. Recently, metallic or metal oxide nanoparticles such as Silver, Gold, Zinc and Titanium have emerged as the most promising and rapidly emerging materials for alternative treatment in wound healing therapies in order to increase efficacy or improve clinical outcome and reduce the likelihood of the emergence of multidrug-resistant and biofilm forming bacteria [14,15]. In particular, numerous research have demonstrated that the high antibacterial potential of metal oxide nanoparticles at low concentrations, their activity against a wide range of bacterial strains [16]. And, their ability to disturb the processes of bacterial DNA amplification, reduces the expression of a wide range of genes that are responsible for virulence, significantly altering the expression of genes responsible for oxidative and general stress. An important feature of metal oxide used in one of the studies is the antibacterial activity against resistant bacterial strains. Certain studies have had a greater focus on how this can be used to improve processes and control infected sites by reducing bacterial infection load, especially in animal wound cases [17]. Their properties such as smaller size and dimension, zeta potential, hydrophobic properties, or the effectiveness of their penetration to deeper levels of tissue, enable ease of application to any type of wound. Previous studies highlight the most recently developed metal and metal oxide nanotechnology-based therapeutic agents and assess the treatment efficacy with emphasis on chronic cutaneous wounds [18].

Among the various metal oxides, the Titanium dioxide nanoparticle (TiO_2-NP) a photoactive metallic nanoparticle has recently shown promise in modern biomedical applications [19]. TiO_2-NP has distinct and unique properties such as an electrical and photocatalytic effect and has a wide range of applications [20]. The most important application area is in biocompatible materials, which have also been used to inactivate bacteria, viruses, and cancer cells. Compared to other antimicrobial agents, TiO_2 in nanoparticle size has received considerable attention due to its stability, safety, and broad-spectrum antibacterial effectiveness as well as being friendly to the environment [21]. Thus, a TiO_2-NP formulation with these properties is expected to create favorable consequences for therapeutic treatment of wounds. Although there are now some reviews exploring the antimicrobial efficacy of TiO_2-NP or wound healing properties, only a few reviews have been published on the topic of the TiO_2-NP formulation specifically used to improve healing of infected wounds in animals [20,22]. Therefore, the purpose of the present study is to provide information about the

 doi:10.20944/preprints202307.0626.v1

characterization, antimicrobial, anti-biofilm forming, and enhance wound healing properties of the TiO_2-NP formulation for the treatment of infected wounds in-vitro and animal model.

2. Materials and Methods

2.1. Preparation and characterization

The TiO_2-NP formulation with sizes ranging from 10 to 100 nm was obtained from Apogee International Company Limited (Bangkok, Thailand). The prepared stock solution was sonicated for 5 mins before being used in each assay. The morphology of TiO_2-NP formulation was observed using transmission electron microscopy (TEM, JEOL JEM-2100, Tokyo, Japan). Certain size and zeta potential were measured by dynamic light scattering (DLS) and with the Zetasizer (Ver. 7.11, Malvern, England), respectively.

2.2. Antimicrobial activities

2.2.1. Agar well diffusion methods

The antimicrobial activity test was carried out in triplicate using the agar well diffusion method described previously by Balouiri et al. [23]. The sterilizing technique was used to prepare Muller-Hinton agar as a standard growth medium (MHA, DifcoTM, USA). Two specific reference bacterial strains (*Staphylococcus aureus*; *S. aureus* ATCC25923 and *Escherichia coli*; *E. coli* ATCC25922) were suspended in 9 ml of 0.85% normal saline solution (NSS) and uniformly spread on MHA with a sterile cotton swab at a concentration of 10^7 – 10^8 CFU/ml (McFarland density = 0.5). Subsequently, wells of 6 millimeters diameter were created with a sterile cork borer. Each well was filled with 35 µl of TiO_2-NP formulation, and wells containing the same volume of solvent (35 µl) were used as a negative control, while a standard antibiotic solution of Gentamicin (a final concentration of 10 µg) were used as the positive controls, incubated at 37°C for 24 hours. Antimicrobial activity of TiO_2-NP formulation was evaluated by observing the appearance of the zone of inhibition and measuring it in millimeters using a Vernier Caliper. The growth inhibition data was obtained in triplicate and presented as the average value along with the standard deviation.

2.2.2. Time-kill kinetic assay

A time-kill kinetic assay with some modifications was performed following the method described by Appiah et al. [24]. In brief, the bacterial suspension was adjusted to a concentration of 10^5 - 10^6 CFU/ml in Muller-Hinton broth (MHB, Oxiod, Thermo Scientific™, England) containing the TiO_2-NP formulation with a concentration equal to the commercial product (Ratio 1:1) and exposed for 0, 5, 15, 30, 60 mins and 4, 6, 12 hours at 37°C. The samples were serially diluted 10-fold in phosphate-buffered saline (PBS) and 100 µl of each sample was inoculated aseptically using the spread plate technique onto standard plate count agar (PCA, Oxiod, Thermo ScientificTM, England). This method was used to calculate the colony forming units (CFU) of bacteria in the samples. The plate with the least dilution that contained a countable (25 - 250 CFU/inoculation) colony forming units was recorded. The average number of colony-forming units in triplicates was calculated as the mean number of colonies.

2.3. Antibiofilm forming activity

The crystal violet assay described by Stepanović et al. [25] with some modifications, was used to quantify biofilm forming activities. Individual wells of a polystyrene 96-well microtiter plate (flat bottom) were filled with 180 µl of tryptic soy broth (TSB, HimediaTM, India) containing 1% glucose and 20 µl of the bacterial suspension (0.5 McFarland scale: 10^7 – 10^8 CFU/ml). In the treatment wells group, 200 µl of TiO_2-NP formulation was diluted from the stock solution to equal the commercial concentration (ratio 1:1), and then 2-fold diluted in TSB before being incubated at 37°C for 24 hours. After incubation, the content 200 µl of each well were discarded by aspiration and the wells were washed three times with phosphate-buffered saline (PBS, pH 7.2) to remove non-adherent cells and

Preprints (www.preprints.org) | NOT PEER-REVIEWED | Posted: 11 July 2023 doi:10.20944/preprints202307.0626.v1

air-dried for 30 to 45 mins. Subsequently, 200 µl of absolute methyl alcohol was added for 20 mins to fix the adhered cells, and then 200 µl of 0.5% crystal violet were added and the plates were incubated in the dark for 15 mins.

After removing the dye solution and washing with sterile distilled water, the attached dye was solubilized with 0.5% (v/v) ethanol and the optical density of the adherent biofilm was measured using an absorbance of crystal violet at a wavelength of 570 nm in a microtiter plate reader [26]. All assays were performed in triplicate and the standard deviation of the mean was calculated. Based on the resulting average optical density (OD) values, the isolates were categorized as non-producing, weak-producing, moderate-producing, and strong-producing for purposes of interpretation. In comparison to the OD values of the negative control, TSB solution without TiO_2-NP formulation was used as the negative control (OD_{NC}), whereby their OD was subtracted from the experimental strains that treated with TiO_2-NP formulation. The biofilm forming abilities were categorized as shown in Table 1.

Table 1. Classification of biofilm formation abilities.

Cut-Off Value Calculation	Biofilm-Formation Abilities
$OD \leq OD_{NC}$	Non-biofilm forming
$OD_{NC} < OD < 2OD_{NC}$	Weak-biofilm forming
$2OD_{NC} < OD < 4OD_{NC}$	Moderate-biofilm forming
$4OD_{NC} < OD$	Strong-biofilm forming

* Abbreviations: OD_{NC}: OD of negative control group, OD: OD of treatment group.

2.4. In-vitro wound healing assay

2.4.1. Cell culture

The porcine kidney cells (PK15, ATCC CCL-33) were propagated and maintained in Dulbecco's Modified Eagle Medium (DMEM) (Gibco, Thermo Fisher Scientific, Waltham, MA, USA) containing 10% (v/v) fetal bovine serum and specific antibiotics (200 IU/ml Penicillin G sodium, 200 g/ml Streptomycin sulfate). Before being used in wound healing assays, cells were seeded into 24-well cell tissue culture plates and incubated at 37°C in a humidified 5% CO_2 incubator for 24 hours to achieve complete spreading of cells and an 80% confluent monolayer.

2.4.2. Scratching wound healing assay

A confluent PK15 monolayer in each well was gently scratched with a sterile 200 µl pipette tip to simulate wounding. The wells were then washed with phosphate buffer saline (PBS) to remove any cellular debris. Following washing, each well was filled with a growth medium (DMEM) containing ten or twenty microliters of TiO_2-NP formulation. As a control, wells containing only the medium were used. The cells were then incubated at 37°C with 5% CO_2 for 24 hours. Following incubation, the scratched cell layers were visualized and photographed at a low magnification (4x) using an Olympus CK40 inverted microscope equipped with a digital camera (Olympus Corporation, Tokyo, Japan). ImageJ/Fiji® software (NIH, Bethesda, MD, USA) was used to quantify scratch of wound areas.

2.5. In-vivo wound healing assay (animal model)

2.5.1. Ethical approval

All experiments were approved by the Institutional Animal Care and Use Committee (Protocol number: 23/2564), Faculty of Medicine, Chiang Mai University, Thailand.

2.5.2. Experimental animals

Nine, six-week-old healthy Mlac: ICR mice (body weight 30 - 40 grams) were included in the experiment. Animals were acclimatized under standard animal laboratory conditions for 7 days prior

 doi:10.20944/preprints202307.0626.v1

to the experiment. All animals in this study were anesthetized with Isoflurane (Isoflurane, USP, Baxter™), which acted as both a sedative and a long-term pain-killer agent. The backs of the mice were shaved, and then sterilized using an alcohol swab. Then, four circular, full-thickness wounds were created aseptically on the dorsal surface of the mice using a sterile 6 millimeters biopsy punch and scissors. The wound sites of all animals were inoculated with 20 µl of *S. aureus* ATCC 25923 at 10^8 CFU/ml (McFarland density = 0.5) to generate infection on wound sites. In this model, wound contraction, early wound healing score and tissue histological were evaluated by using a semi-quantitative scoring system. Bacterial data from the wound were collected 24 hours after bacterial inoculation as the number of colony forming units per milliliter (CFU/ml) investigated by using drop plate techniques. The mean ± standard was calculated and set as the starting point for wound colonization. The animals were randomly divided into three groups, each consisting of 3 mice: group I, a negative control group, which received 20 µl of 0.85% NSS; group II, a positive control group, which received 20 µl of iodine solution (1% active iodine); and group III, a treatment group, which received 20 µl of TiO_2-NP formulation. Before application of the solution onto the mice, the wounds were disinfected with 0.85% NSS to clean the wound surface and remove any debris. Early wound healing score (EHS), percentage of wound contraction and bacterial colonization were assessed for all group members at a terminal time point on days 1, 3, 6, 9, and 14 after wound creation.

2.5.3. Early wound healing score (EHS)

The physical appearance of wound healing was monitored by taking digital photographs to determine the early wound healing score (EHS). The EHS system comprises three parameters, including clinical signs of re-epithelialization (CSR), clinical signs of hemostasis (CSH), and clinical signs of inflammation (CSI). The summation of the points for these three parameters generated the EHS. According to Marini et al. [27], the optimal wound healing outcome is characterized by an ESH score of 10 points, whereas the lowest wound healing outcome is represented by a score of 0 points. The descriptions of early wound healing scoring system are shown in Table 2.

Table 2. Early wound healing score descriptions.

Parameter	Descriptions	Score
CSR	Merged surgical wound margins	6
	Surgical wound margins in contact	3
	Visible distance between surgical wound margins	0
CSH	Absence of fibrin on the surgical wound margins	2
	Presence of fibrin on the surgical wound margins	1
	Bleeding at the surgical wound margins	0
CSI	Absence of redness along the surgical wound diameter	2
	Redness involve < 50% of the diameter	1
	Redness involve > 50% of the diameter and/or pronounced swelling	0

* Abbreviations: CSR: clinical signs of re-epithelialization, CSH: clinical signs of hemostasis, CSI: clinical signs of inflammation.

2.5.4. Wound microbial assay

The modified drop plate technique described by Naghili et al. [28] was used to determine the total amount of bacteria present on the wound sites. Before collecting a sample from each wound site, the wounds were cleaned by scrubbing with 0.85% NSS to remove any debris. Then, the wound surface was swabbed using a sterile cotton swab that was saturated with phosphate buffer saline (PBS). To obtain a homogeneous suspension, a volume of 100 µl of the sample solution was mixed with 900 µl of sterile PBS. The sample suspension was subsequently subjected to a 10-fold serial dilution to achieve a final concentration range of 10^{-1} to 10^{-5}. A volume of 10 µl of each dilution was carefully placed onto the plate count agar (PCA). The plates were incubated at 37°C for 24 hours.

Preprints (www.preprints.org) | NOT PEER-REVIEWED | Posted: 11 July 2023 doi:10.20944/preprints202307.0626.v1

After incubation, the colonies were counted and the average number of colonies was determined as the minimum dilution that contained a countable number of colonies (25 - 250 CFU/inoculation). The results were expressed in CFU/ml.

2.5.5. Wound contraction

The size of each wound area was measured using Vernier Calipers. The percentage of wound contraction was calculated using the following formula.

$$WC = [(A0 – At)/At] \times 100$$

where W_C is the percentage of wound contraction, A_0 is the original wound area, and A_t is the area of wound at the time of measurement (days 0, 3, 6, 9 and 14 post wound creation).

2.5.6. Tissue collection and histological analysis

The skin samples from each group were taken on days 0 and 14 after wound creation from the periphery of the wound, along with normal skin and fragments of infected skin. Samples were fixed in 10% buffered formalin, processed by dehydration and embedded in paraffin blocks. Then, samples in a paraffin block were sectioned into 3 µm-thick sections and stained with Hematoxylin and Eosin (H&E) stains. Wound healing scores and histological changes in each sample were photographed and observed under a light microscope. The study used a semi-quantitative scoring system based on an ordinal scale with four histological parameters: granulation tissue amount, inflammatory infiltrate, collagen fiber orientation, and collagen pattern. The scoring system was previously established by Sultana and Santos [29,30] and is presented in Table 3. The overall healing score for each group was calculated by summing the individual criterion scores. Lower scores indicated poor healing status (8 - 11), while middle (12 - 15) and good (16 - 19) scores indicated intermediate and good healing status, respectively.

Table 3. Histological parameters used to assess and calculate wound healing state.

Histological Parameters	Scoring System	Histological Grading
Amount of granulation tissue	Profound	1
	Moderate	2
	Scanty	3
	Absent	4
Inflammatory infiltrate	Plenty	1
	Moderate	2
	A few	4
Collagen fiber orientation	Vertical	1
	Mixed	2
	Horizontal	4
Pattern of collagen	Reticular	1
	Mixed	2
	Fascicle	4

2.6. Statistical analysis

Statistical analysis was conducted using ANOVA and Kruskal-Wallis tests for parametric and non-parametric data, respectively. The purpose was to assess differences between groups on each day, including wound contraction rate, bacterial concentration, early wound healing score, and histopathology parameter score. Post-hoc multiple comparison tests were conducted to identify significant differences between groups with a significance level of 0.05, following ANOVA and Kruskal-Wallis tests. The paired T-test was used to compare the starting day (Day 0) with the

Preprints (www.preprints.org) | NOT PEER-REVIEWED | Posted: 11 July 2023 doi:10.20944/preprints202307.0626.v1

treatment days (Day 3, 6, 9, and 14) following surgical procedures. Violin plots were generated using ggpubr package in R software version 3.5.1/R studio version 1.1.456.

3. Results

3.1. Characterization of TiO2-NP formulation

The Malvern Zetasizer determined that the particle size of the TiO_2-NP formulation was 383.1 ± 23.05 nm (PDI=0.931) and the negative zeta potential was 19.27 ± 4.65 mV (Figure 1). The transmission electron microscope (TEM) revealed the agglomeration of two distinct morphologies of particles, including spherical and polygonal shapes, with particle sizes ranging from 50 to 100 nm (Figure 2).

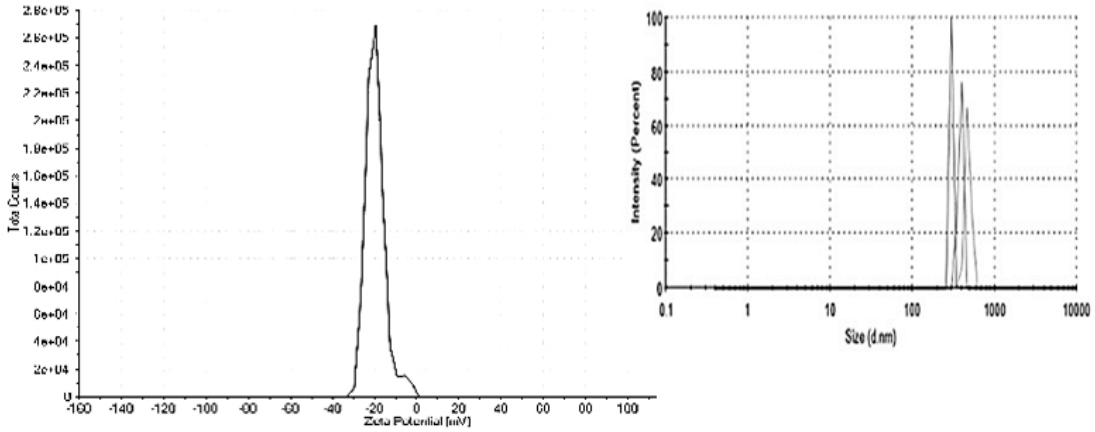

Figure 1. (a) and **(b).** shows the zeta potential and mean particle size of TiO_2-NP.

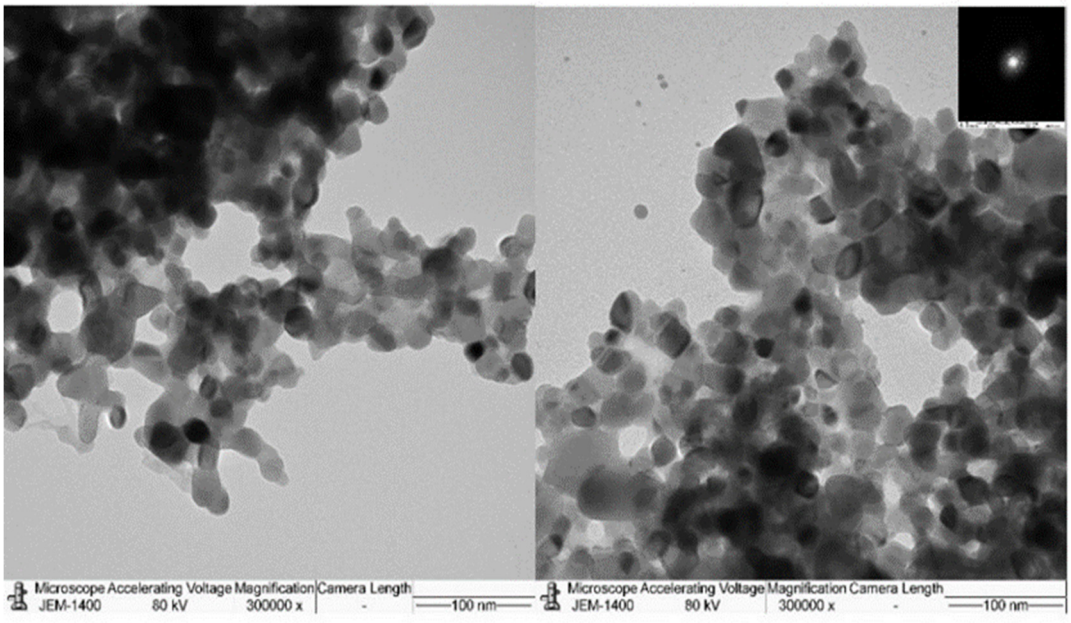

Figure 2. Transmission electron microscopy (TEM) reveals the morphology of the TiO_2-NP.

3.2. Antimicrobial and Antibiofilm forming activities

The results indicated that the TiO_2-NP formulation has antibacterial properties against *S. aureus* ATCC 25923 and *E. coli* ATCC 25922. In comparison to gram stain bacteria, gram-negative bacteria appear to be more susceptible to almost all treatments, except positive control group such as

Preprints (www.preprints.org) | NOT PEER-REVIEWED | Posted: 11 July 2023 doi:10.20944/preprints202307.0626.v1

Gentamycin. Gentamycin was the most effective agent against both microorganisms tested, whereas there were no statistically significant differences in zones of inhibition between TiO_2-NP formulation, Ag-NP formulation (Nano Care: Silver nano formulation, Bangkok, Thailand), and Iodine solution (Betadine, Bangkok, Thailand) against *S. aureus*, with the exception of the Ag-NP formulation. Ag-NP formulation has high efficacy against *E. coli* (Table 4).

Table 4. Zones of inhibition of metal and metal-oxide nano formulations against reference bacterial strains.

Bacteria	Inhibition Zones (mm)				
	N	TiO_2-NP	Ag-NP	Iodine Solution	Gentamycin
S. aureus	3	20.00 ± 5.42	20.12 ± 0.18	22.23 ± 0.24	31.75 ± 0.37*
E. coli	3	24.00 ± 1.91	29.50 ± 0.50*	24.51 ± 0.43	30.50 ± 0.75*

* Asterisks indicate significant differences ($p < 0.05$).

Bacteriostatic and bactericidal effects were evaluated using time-kill assays. Bacterial reductions of three logs of CFU/ml or greater from the initial inoculation concentration are considered bactericidal [31]. The results show that the TiO_2-NP formulation had a bactericidal effect, lowering the starting log CFU/ml by more than 3 logs after 10 mins against *E. coli* and after 6 hours against *S. aureus*. No measurable growth of *E. coli* was observed 15 mins after inoculation and lasted for 12 hours, whereas no measurable growth of *S. aureus* was observed at the 12-hour time point (Figure 3A-B).

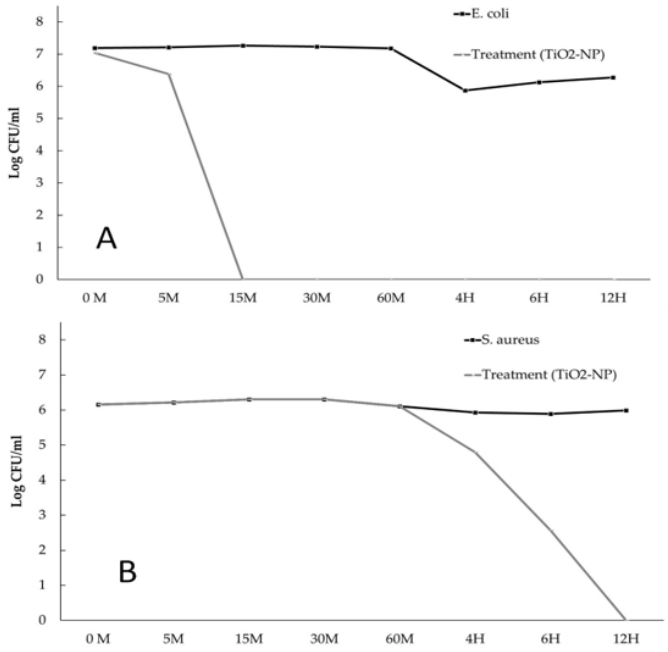

Figure 3. The time kill kinetic profiles of TiO_2-NP formulation against *E. coli* (**A**) and *S. aureus* (**B**).

The biofilm forming ability was measured using the crystal violet method. All isolates tested were biofilm producers. Among the 2 reference bacterial strains, *S. aureus* was classified as a strong biofilm former ($OD > 4OD_{NC}$), whereas *E. coli* was classified as a weak-producing biofilm former ($OD_{NC} < OD \leq 2\ OD_{NC}$). The TiO_2-NP formulation acted as an antibiofilm agent in all reference strains causing differences in biofilm formation and lower inhibition of initial cell adhesion compared to the negative control. The treatment of *S. aureus* and *E. coli* with TiO_2-NP formulation for 24 hours reduced biofilm formation by more than 99% (Figure 4).

Preprints (www.preprints.org) | NOT PEER-REVIEWED | Posted: 11 July 2023 doi:10.20944/preprints202307.0626.v1

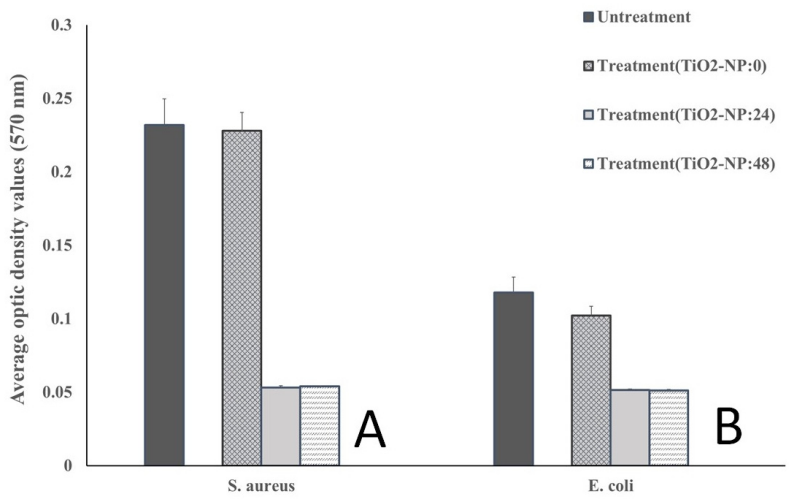

Figure 4. Biofilm formation ability of *S. aureus* (A) and *E. coli* (B) at different times of TiO_2-NP formulation exposure compared with the untreated group.

3.3. Wound healing assay

3.3.1. In-vitro

According to the findings, the TiO_2-NP formulation has an effect on the growth of swine kidney cells (PK15) in the in-vitro scratch wound healing assay. A representation of both concentrations of TiO_2-NP formulation significantly enhanced the proliferation and migration of the cells compared to the untreated control cells in a dose-dependent manner ($p = 0.0016$). Figure 5 shows that without TiO_2-NP formulation supplementation, wound edges widened in comparison to those with TiO_2-NP formulation supplementation at 10 µl and 20 µl. In comparison to the untreated control (32,033 μm^2), TiO_2-NP supplementation at 10 µl and 20 µl resulted in a median wound area of 21,646 μm^2 and 21,887 μm^2, respectively.

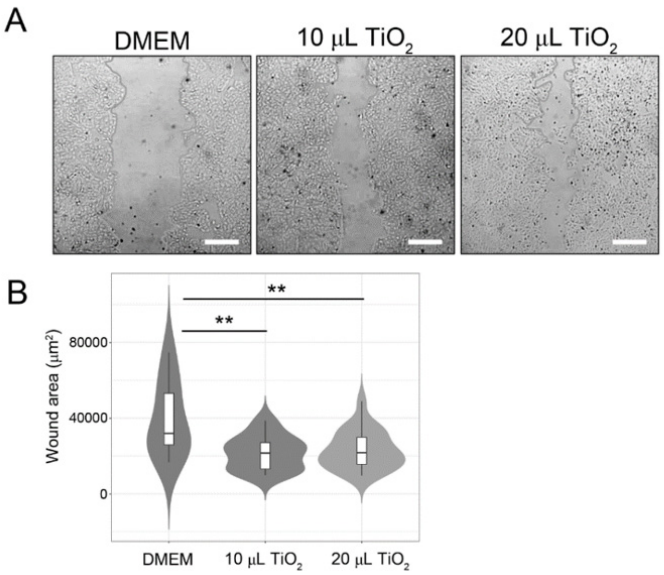

Figure 5. In-vitro scratch wound healing assays demonstrating that cell migration into the cell-free region (A) is significantly different between the 10 and 20 µl as compared to the negative controls

Preprints (www.preprints.org) | NOT PEER-REVIEWED | Posted: 11 July 2023 doi:10.20944/preprints202307.0626.v1

(DMEM). (B) A summary bar graph illustrating the percentage of wound closure at the indicated time points during the scratch wound. assay (**< 0.01 compare with control).

3.3.2. In-vivo (animal model)

Each experiment was conducted on surgical wounds infected with *S. aureus*. Figure 6 illustrates the number of bacteria in CFU/ml for each treatment group with different durations, including the negative control (Group I: 0.85% NSS), the treatment (Group II: TiO_2-NP formulation), and the positive control (Group III: Iodine solution), from Day 1 to Day 14. The results indicate that there is no difference in the number of bacteria between groups ($p > 0.05$). Nonetheless, it was found that the bacterial load decreased in all groups from the time of exposure.

The macroscopic evaluation of the wound did not show evidence of any purulent exudate in any of the wounded animals during study period. However, it was possible to observe mild inflammatory signs with a serous exudation, characterized by redness, and swelling at the edges of the wound on Day 0. In all groups, the wound healing exhibited a reduction in clinical signs after the surgery, as well as an increase in the rate of wound contraction and a decrease in wound area. To evaluate the physical appearance, we used the early wound healing score (EHS) and carried out semi-quantitative scoring comparisons between groups on different observation days.

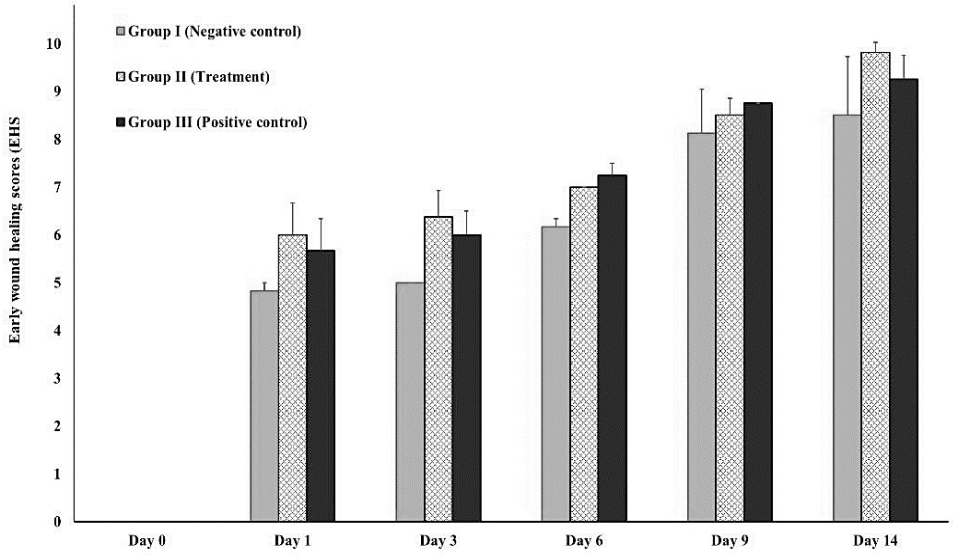

Figure 6. Total bacterial count measured by log CFU/ml in each experiment.

The EHS was determined for the wounds in the early stage of healing, starting at 24 hours after surgical approach and inoculation with *S. aureus* infection (Figure 7). The mean EHS values of the negative control, treatment, and positive control groups were 4.83 ± 0.167, 6.00 ± 0.67, and 5.67 ± 0.67, respectively. On Day 14, the treatment groups exhibited the highest EHS score of 9.81 ± 0.21 followed by the positive control group with a score of 9.25 ± 0.50 and the negative control group scoring 8.50 ± 1.22. On days 3 and 6, the treatment group showed statistically significant better scores (6.38 ± 0.96 and 7.00 ± 0.00) in comparison to the negative control groups (5.00 ± 0.00 and 6.17 ± 0.39) of $p = 0.00128$ and $p = 0.000001$, respectively.

Preprints (www.preprints.org) | NOT PEER-REVIEWED | Posted: 11 July 2023 doi:10.20944/preprints202307.0626.v1

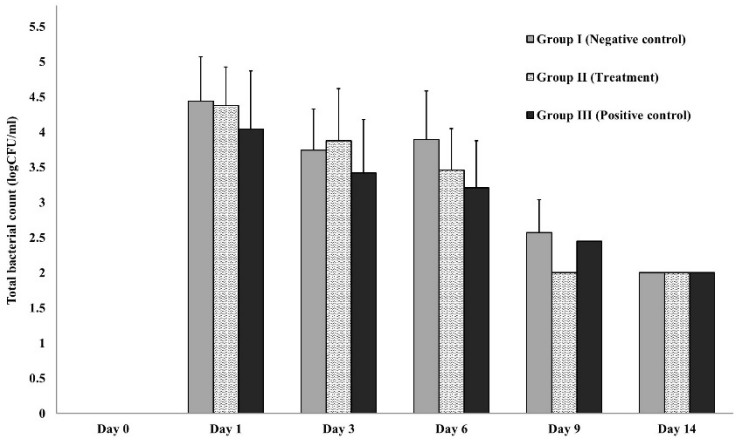

Figure 7. Early wound healing score (EHS) on Day 1, 3, 6, 9, and 14 compared to Day 0.

The percentages of the wound contraction induced by topical application of the TiO_2-NP formulation, 0.85% NSS and Iodine solution are shown in Figure 8(A). Results demonstrate that treatment of wounds with the TiO_2-NP formulation induced a significant ($p < 0.05$) improvement in the percentage of wound contraction (91.25 ± 2.50) compared to the negative control group treated with 0.85% NSS (86.50 ± 0.71). Starting on the third day of treatment, the TiO_2-NP formulation showed significant wound contraction compared to the negative control group. The TiO_2-NP formulation also showed better wound contraction than iodine solution from three to fourteen days after wounding, although the difference was not statistically significant.

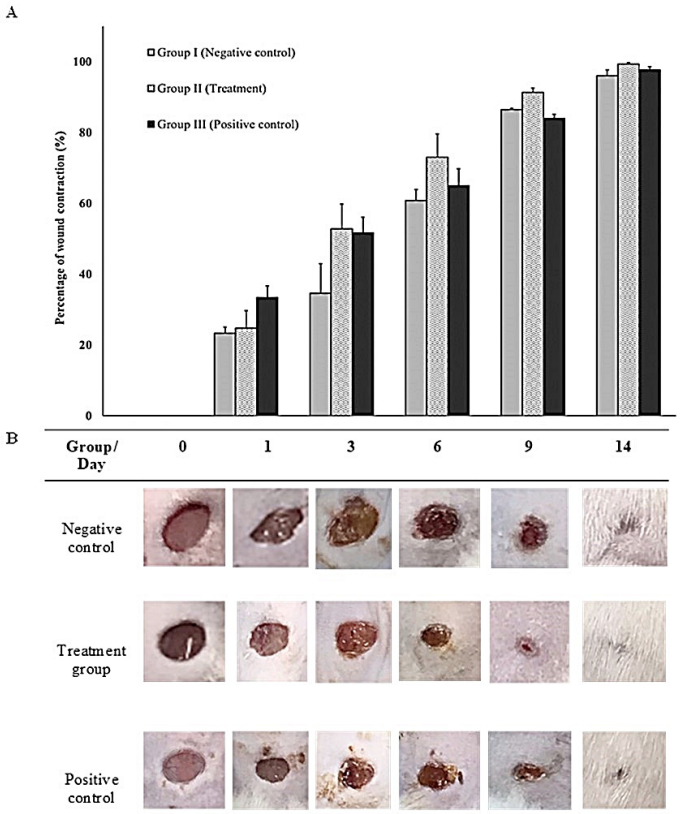

Figure 8. (A) and (B). Wound appearance and contraction on Days 0, 1, 3, 6, 9, and 14 showing comparison between groups (Group I: negative control (0.85% NSS), Group II: treatment (TiO_2-NP formulation), and Group III: positive control (Iodine solution).

Preprints (www.preprints.org) | NOT PEER-REVIEWED | Posted: 11 July 2023 doi:10.20944/preprints202307.0626.v1

The microscopic evaluation of the wounds was carried out by taking a standardized biopsy for histopathological analysis which encompassed the whole wound, including the edges. Hematoxylin and Eosin (H&E), a commonly used staining method for dermatopathology, was employed for the descriptive analysis of wound healing parameters, including the inflammatory infiltrate, tissue granulation, primary fibrous scarring, and the epithelialization process. A comparative analysis was performed between the groups on days 0 and 14. The sectioning of the skin and subcutaneous samples obtained after surgical intervention and treatment in all groups (Group I: negative control group, Group II: treatment group, Group III: positive control group,) revealed multifocal accumulation of the inflammatory cells predominantly composed of non-degenerated neutrophils, with fewer degenerated neutrophils, lymphocytes, macrophages, and foci of necrosis.

The comparison of histological scoring between Day 0 and Day 14 was performed by three examiners who were blinded to the group information during all histological analyses. The parameters evaluated included the amount of granulation tissue, pattern of collagen, inflammatory infiltrate, and collagen fiber orientation. On Day 14, the treatment group that received TiO_2-NP formulation showed a higher score for the amount of granulation tissue (2.75 ± 0.25) compared to the negative and positive control groups (2.25 ± 0.25, 2.25 ± 0.48). Additionally, the treatment group also showed the highest score for the pattern of collagen (3.00 ± 0.00) with remarkable vertical collagen formation. However, the inflammatory infiltrate and collagen fiber orientation were lower in the treatment group. In the positive control group, which was exposed with Iodine solution, the histological analysis revealed a mixed pattern of collagen fiber formation, infiltration of a moderate number of mononuclear cells (MN) and the presence of foci of ulceration and fibrin formation mixed with increasing granulation tissue. On Day 14, there was a statistically significant difference between treatment and control group as regards the pattern of collagen as assessed using the Kruskal-Wallis test ($p = 0.045$). The pairwise Dunn's test between groups showed that only the difference between the negative control group (0.85% NSS) and treatment group (TiO_2-NP) was significant ($p = 0.0417$). However, there was no significant difference between collagen parameters, including number and pattern of collagen fibers among any groups on Day 0 and Day14 (Figure 9).

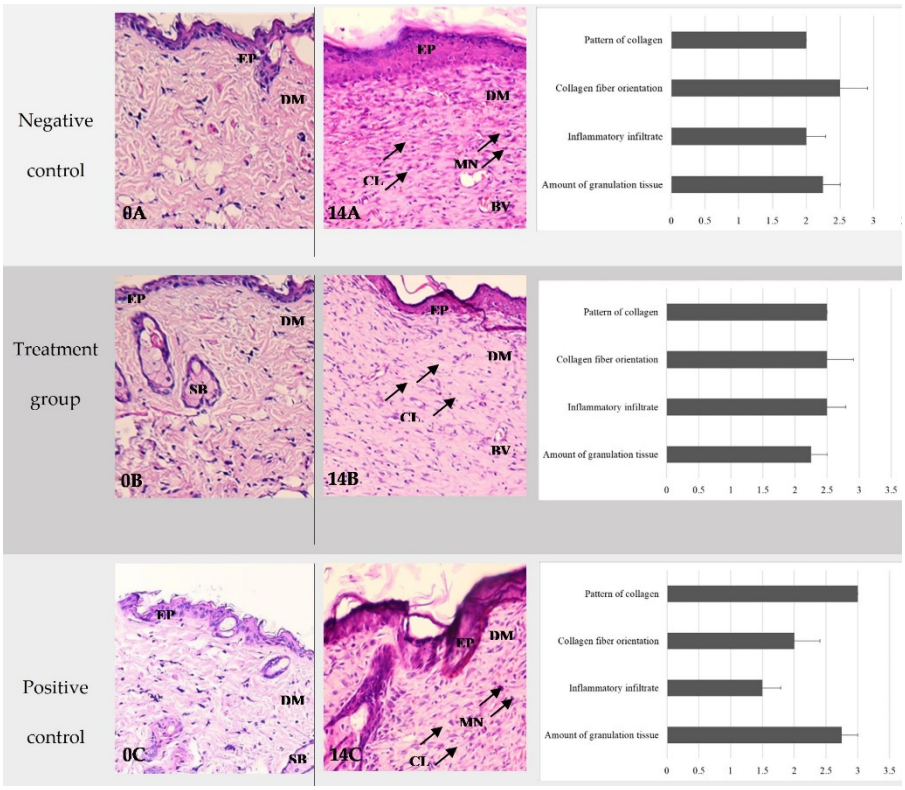

Figure 9. Representative histopathological sections stained with H&E of wound healing on Days 0 and 14 showing comparisons between groups (A: negative control group; B: treatment group (TiO_2-

 doi:10.20944/preprints202307.0626.v1

NP formulation); C: positive control group). Note the thin epidermis and dermis above the abundant subcutaneous layer on Day 0 (A–C) compared with Day 14 (A–C). The H&E staining shows collagen fibers-stained pale pink, cytoplasm stained purple, nuclei stained blue, and red blood cells-stained cherry red. The negative control had the thickest layer of epithelium compared to the other groups and showed remarkable vertical collagen formation (14A). The TiO2 NP formulation was randomly infiltrated with mononuclear cells (MN) and mainly vertical collagen formation (14B). The positive control demonstrates a mixed pattern of collagen fiber formation, infiltration of a moderate number of mononuclear cells (MN), and granulation tissue (14C). The wound exhibits a few to moderate numbers of infiltrating inflammatory cells, the majority of which are neutrophils, and a small number of macrophages and lymphocytes with foci of necrosis, ulceration, and fibrin formation (0A, 0B, 0C). Abbreviations: H&E, Hematoxyline-Eosin; EP, Epidermis, DM; Dermis, SB; Sebaceous gland, BV; Blood vessel, MN; Mononuclear cell infiltration, CL; Collagen fiber orientation.

4. Discussion

In this study, the average particle size of the TiO_2-NP formulation determined by DLS was 383.1 ± 23.05 nm, and the zeta potential value was -19.27 ± 4.65 mV. The zeta potential is a significant and readily apparent indicator of colloidal dispersion stability and a major factor in the initial adsorption of nanoparticles on the cell membrane [13]. The magnitude of the zeta potential in dispersion indicates the degree of electrostatic repulsion between adjacent, similarly charged particles. In general, a zeta potential magnitude of +30 or -30 mV is considered the minimum value to indicate a stable suspension. The zeta potential of the TiO_2-NP formulation obtained in this study is less than 30 mV, resulting in incipient stability and less potential force to prevent particle aggregation and flocculation [32]. As shown by the TEM the TiO_2-NP formulation was approximately spherical in form with uneven borders and few aggregations (Figure 2), which relates to a low level of negative zeta potential value.

The structural and physicochemical properties, including size, shape, zeta potential and surface charge of metal oxide nanoparticles (MONP) could affect biological function. The antimicrobial activity of MONP would become more significant at nano level owing to the increased surface area, enabling differentiation between bacterial cells and mammalian cells and can provide long term antibacterial and biofilm prevention. The particles sizes of TiO_2-NP determined by TEM ranged from 10 to 50 nm, which is typical for nanomaterials that are effective antimicrobial agents. Previous studies demonstrated that synthesized TiO_2-NP with sizes ranging from 28 to 54 nm are capable of passing through *S. aureus*, while sizes ranging from 62 to 74 nm are able to pass through and inhibit *E. coli* and *P. aeruginosa* [33]. TiO_2-NP's antibacterial mechanisms includes cell wall damage caused by electrostatic interaction, oxidative stress caused by the generation of reactive oxygen species (ROS), and disruption of protein functions and cell structures caused by metal cation release, which leads to cell death [34].

The results indicate that the TiO_2-NP formulation exhibits antibacterial effects against *S. aureus* ATCC 25923 and *E. coli* ATCC 25922. Similar to previous research, TiO_2-NP is an interesting antimicrobial substance due to their outstanding antibacterial capabilities against a wide spectrum of gram-positive and gram-negative bacteria. Gram-negative bacteria exhibit greater susceptibility to almost all of the treatments in comparison to gram-positive bacteria. The observed phenomenon may be attributed to the variation in thickness of bacterial cell walls, which ranges from 20 - 80 nm in gram-positive and 1.5 - 10 nm in gram-negative bacteria [35]. Consequently, the susceptibility of bacterial cells to peroxidation induced by reactive oxygen species (ROS) generated by TiO_2-NP is increased, allowing for the penetration and destruction of cellular structures by small particles such as nanoparticles [36]. Furthermore, previous reports have documented that the cell walls of *E. coli* (gram-negative bacterial group) comprise lipo-polysaccharide, phosphatidyl-ethanolamine, and peptidoglycan and is susceptible to peroxidation induced by TiO_2. Consequently, it is anticipated that the impact of TiO_2-NP will exhibit slight variations depending on the type of microorganism involved [37].

The time-kill kinetic assay revealed similar antibacterial results, specifically after 10 mins and 6 hours, the TiO_2-NP formulation reduced *E. coli* and *S. aureus* by more than 3 logs. No measurable

growth of *E. coli* was observed 15 mins after inoculation an effect which persisted for 12 hours, while no measurable growth of *S. aureus* was observed at the 12-hour interval. Pulgarin et al. [38] have reported comparable findings regarding the effectiveness of TiO_2 thin film coated on the PVC substrate against *E. coli*. The bacterial count was observed to decrease from 6.90×10^9 to 5.00×10^2 CFU/ml within 60 mins, indicating that over 99% of the *E. coli* population was eliminated. Furthermore, Di Pilato's study [39] demonstrated that the time kill kinetics of *Staphylococcus* group organisms with significant biofilm formation, such as *S. aureus* and *S. epidermidis*, increased with exposure duration. Biofilm formation is a complex process that involves the attachment of microorganisms to surfaces and the production of an extracellular matrix. The matrix provides protection against environmental stressors such as antibiotics and host immune responses. *S. aureus* and *S. epidermidis* are two organisms that are known to form biofilms, and their ability to do so increases with exposure duration. This is concerning because biofilm formation is a significant factor in the increase in antibiotic resistant bacteria. In fact, the biofilm produced by *S. aureus* may be the cause of increased antimicrobial resistance in wound sites [40], which can lead to serious infections that are difficult to treat. Therefore, understanding the mechanisms of biofilm formation and finding new ways to disrupt it may be key in combating antibiotic resistance and improving patient outcomes.

We found that the TiO_2-NP formulation acted as an antibiofilm agent in all reference strains, causing differences in biofilm formation and lowering initial cell adhesion when compared with the negative control in 24 hours. Similar to the findings published by Carrouel and Viennot, who observed that adding metal oxide, specifically TiO_2, to toothpastes and mouthwashes increased their antibacterial effectiveness against dental plaque-causing microbes [41]. Furthermore, Jesline et al. [13] demonstrated that TiO_2-NP were effective against Methicillin Resistant *Staphylococcus aureus* (MRSA) and *E. coli* by reducing biofilm formation by 40 - 50% [42]. TiO_2-NP formulation can reduce the adhesion of bacteria and inhibit biofilms, primarily due to the generation of ROS and lipid oxidation on the cell wall membrane due to exposure to TiO_2-NP leads to the destruction of bacterial inside the biofilm. In addition, the interaction between TiO_2-NP and biofilm is determined by their electrostatic characteristics. The positive charge of the bacterial biofilm matrix can interact with negatively charged metal ions and organic compounds through electrostatic forces. Some studies have recently revealed that TiO_2-NP has promising cell growth promoting characteristics in the wound healing process [43,44].

The present study also used an animal model to assess the in-vivo efficacy of a TiO_2-NP formulation for the treatment of *S. aureus*-infected wounds. The wounds in all groups showed only mild inflammation with serous exudation at the wound edges, which is a normal part of the healing process. The results show that at the time of exposure, the bacterial load decreased in all groups, and there is no difference in the number of bacteria between groups ($p > 0.05$). This can be explained due to all healthy mice used in this study having a normal defense mechanism to eliminate pathogens and reduce the bacterial load to the normal level of commensal organisms on the skin. These findings add weight to previous studies that found the health and immune status of a patient have a significant impact on the bacterial diversity and population of the cutaneous microbiota [45].

The endpoint of a successful treatment is complete and permanent wound closure. In clinical practice, the rate of change in the surface area of the wound, also known as the wound healing rate, is the best way to quantify the healing progress. In this study, the results showed the highest EHS score (9.81 ± 0.21) in the treatment group on Day 14 and showed better scores, especially on Days 3 and 6, that were higher than in the negative control groups. Generally, the hemostatic reaction occurs immediately after the wound appears, with vascular constriction and fibrin clot formation. Once bleeding is controlled, inflammatory cells migrate into the wound and promote the inflammatory phase, which is characterized by the sequential infiltration of mononuclear cells such as neutrophils, macrophages, and lymphocytes. Our studies have shown that the TiO_2-NP formulation was able to enhance cell migration, which is a critical component of the wound healing process, especially in the inflammatory reaction stage. Proliferation occurs at the end of the inflammatory response, during which inflammatory cells convey chemotactic information to stimulate the migration of fibroblasts to

the wound. These fibroblasts then deposit in the extracellular matrix, marking the beginning of the formation of granulation tissue. The formation of granulation tissue can typically be observed within 3 - 5 days after the injury, and our results have shown that the group treated with TiO_2-NP formulation had a higher EHS score during the process of formation of the granulation tissue. In addition, abundant extracellular matrix has accumulated in the myofibroblast phenotype, which is associated with a statistically significant difference in the percentage of wound contraction between the groups.

Histological analysis showed that the treatment group receiving the TiO_2-NP formulation had significantly higher scores for granulation tissue and collagen patterns in comparison to the negative and positive control groups at the end of the study. Fibroblast proliferation was detected in the dermis and subcutaneous tissue, resulting in collagen deposition and evidence of vertical formation of collagen. The arrangement and orientation of collagen plays a crucial role during the remodeling phase, which influences the appearance of the final scar after wound closure. The group treated with TiO_2-NP formulation exhibited a vertical collagen orientation, whereas the Iodine solution group displayed a mixed pattern of collagen fiber formation, suggesting that the main difference between scarred and unwounded skin appears to be the density, uniformity, size, and orientation of the collagen fibrils. Collagen and elastic fibers exhibit a correlation in density along two directions, namely horizontal and vertical. The presence of a mixed pattern of collagen fibers in the Iodine solution group is characterized by non-uniformity and low density, which can potentially contribute to the appearance of unhealed skin [46]. The histological analysis of the healed wound tissues on day 14 was consistent with the visual observation and grading. This suggests that the TiO_2-NP formulation is an acceptable wound healing agent, with outcomes comparable to the positive control group, and superior to the negative control group.

5. Conclusions

The results of the study suggest that TiO_2-NP formulation is a highly effective antimicrobial and antibiofilm agent. These properties make it a promising candidate for use in medical applications, particularly with regard to wound healing. The scratch wound healing assay and animal model both showed increased cell migration rates with the use of TiO_2-NP, indicating its potential to accelerate the healing process. With further research and development, TiO_2-NP could become a valuable tool in the fight against bacterial infections and in promoting tissue regeneration. Its unique properties make it a compelling alternative to traditional antibiotics and wound care treatments.

Author Contributions: Conceptualization, N.P. and W.C.; methodology, Y.T. and A.K.; investigation, W.S. and A.K.; writing-original draft preparation, N.P.; writing-review and editing, P.C. and W.C.; visualization, M.I.; supervision, S.P. and W.C.; project administration, W.C.; all authors have read and agreed to the published version of the manuscripts.

Funding: This research was supported by the research grant of Research and Researcher for Industries (RRI64): grant number [N4160338], and the Apogee International Company Limited, Bangkok, Thailand.

Institutional Review Board Statement: The animal study protocol was approved by the Institutional Animal Care and Use Committee (Protocol number: 23/2564), Faculty of Medicine, Chiang Mai University, Thailand.

Informed Consent Statement: Not applicable.

Data Availability Statement: The data presented in this study are available upon request from the corresponding author. The data are not publicly available due to the privacy policy of the authors' institution.

Acknowledgments: The author is most sincerely grateful to the Central of Veterinary Diagnostic, Faculty of Veterinary Medicine, Chiang Mai University and the team of technicians, including Anyaphat Srithanasuwan, Kornravee Photichai, and Benyaporn Sornpet for their support in laboratory activities.

Conflicts of Interest: The authors declare no conflict of interest.

References

1. Puca, V.; Marulli, R.Z.; Grande, R.; Vitale, I.; Niro, A.; Molinaro, G.; Prezioso, S.; Muraro, R.; Di Giovanni, P. Microbial species isolated from infected wounds and antimicrobial resistance analysis: Data emerging from a three-years retrospective study. *Antibiotics* (Basel). **2021**, 10.
2. Roy, S.; Ahmed, M.U.; Uddin, B.M.M.; Ratan, Z.A.; Rajawat, M.; Mehta, V.; Zaman, S.B.. Evaluation of antibiotic susceptibility in wound infections: A pilot study from Bangladesh. *F1000Res 6*. **2017**, 2103.
3. Frykberg, R.G.; Banks, J. Challenges in the treatment of chronic wounds. *Adv. Wound Care (New Rochelle)*. **2015**, 4, 560-582.
4. Kadam, S.; Nadkarni, S.; Lele, J.; Sakhalkar, S.; Mokashi, P.; Kaushik, K.S. Bioengineered platforms for chronic wound infection studies: How can we make them more human-relevant? *Front. Bioeng*. **2019**, 7.
5. Gueltzow, M.; Khalilpour, P.; Kolbe, K.; Zoellner, Y. Budget impact of antimicrobial wound dressings in the treatment of venous leg ulcers in the German outpatient care sector: A budget impact analysis. *J. Mark Access Health Policy*. **2018,** 6, 1527654.
6. Norman, R.E.; Gibb, M.; Dyer, A.; Prentice, J.; Yelland, S.; Cheng, Q.; Lazzarini, P.A.; Carville, K.; Innes-Walker, K.; Finlayson, K.; Edwards, H.; Burn, E.; Graves, N. Improved wound management at lower cost: A sensible goal for Australia. *Int. Wound J*. **2016**, 13, 303-316.
7. Bowler, P.G.; Welsby, S.; Towers, V.; Booth, R.; Hogarth, A.; Rowlands, V.; Joseph, A.; Jones, S.A. Multidrug-resistant organisms, wounds and topical antimicrobial protection. *Int. Wound J*. **2012,** 9, 387-396.
8. Corsini, C.M.M.; Silva, V.O.; Carvalho, O.V.; Sepúlveda, R.V.; Valente, F.; Reis, E.; Moreira, M.; Silva, A.; Borges, A. emergence of multidrug-resistant bacteria isolated from surgical site infection in dogs and cats. *Arq. Med. Vet*. **2020**, 72, 1213-1220.
9. Li, J.; Cao, J.; Zhu, Y.-G.; Chen, Q.; Shen, F.; Wu, Y.; Xu, S.; Fan, H.; Da, G.; Huang, R.-j.; Wang, J.; de Jesus A.L.; Morawska, L.; Chan, C.K.; Peccia, J.; Yao, M. Global survey of antibiotic resistance genes in air. *Environ. Sci. amp; Technol*. **2018**, 52, 10975-10984.
10. Wee, B.A.; Muloi, D.M.; van Bunnik, B.A.D. Quantifying the transmission of antimicrobial resistance at the human and livestock interface with genomics. *Clin. Microbiol. Infect*. **2020,** 26, 1612-1616.
11. Uruén, C.; Chopo-Escuin, G.; Tommassen, J.; Mainar-Jaime, R.C.; Arenas, J. Biofilms as promoters of bacterial antibiotic resistance and tolerance. *Antibiotics* (Basel). **2020**, 10.
12. Shkodenko, L.; Kassirov, I.; Koshel, E. Metal oxide nanoparticles against bacterial biofilms: Perspectives and limitations. *Microorganisms*. **2020**, 8.
13. Jesline, A.; John, N.P.; Narayanan, P.M.; Vani, C.; Murugan, S. Antimicrobial activity of Zinc and Titanium dioxide nanoparticles against biofilm-producing methicillin-resistant Staphylococcus aureus. *Appl. Nanosci*. **2015**, 5, 157-162.
14. Rajendran, N.K.; Kumar, S.S.D.; Houreld, N.N.; Abrahamse, H. A review on nanoparticle-based treatment for wound healing. *J. Drug Deliv. Sci. Technol*. **2018**, 44, 421-430.
15. Ziental, D.; Czarczynska-Goslinska, B.; Mlynarczyk, D.T.; Glowacka-Sobotta, A.; Stanisz, B.; Goslinski, T.; Sobotta, L. Titanium dioxide nanoparticles: Prospects and applications in medicine. *Nanomaterials* (Basel). **2020**, 10.
16. Gudkov, S.V.; Burmistrov, D.E.; Serov, D.A.; Rebezov, M.B.; Semenova, A.A.; Lisitsyn, A.B.; A mini review of antibacterial properties of ZnO nanoparticles. *Front. Phys*. **2021**, 9.
17. Barroso, A.; Mestre, H.; Ascenso, A.; Simões, S.; Reis, C. Nanomaterials in wound healing: From material sciences to wound healing applications. *Nano. Select*. **2020**, 1, 443-460.
18. Mallick, S.; Nag, M.; Lahiri, D.; Pandit, S.; Sarkar, T.; Pati, S.; Nirmal, N. P.; Edinur, H. A.; Kari, Z. A.; Ahmad Mohd Zain M. R.; Ray R. R. Engineered nanotechnology: An effective therapeutic platform for the chronic cutaneous wound. *Nanomaterials*. **2022,** 12(5), 778.
19. Carol López de, D.; Matias Guerrero, C.; Fernanda, B.M.; Camilo, S.; Maria José, G. Antimicrobial effect of Titanium dioxide nanoparticles: Antimicrobial resistance. *Intech. Open. Rijeka,* **2020;** *Ch. 5.*
20. Nikpasand, A.; Parvizi, M.R. Evaluation of the effect of Titatnium dioxide nanoparticles/gelatin composite on infected skin wound Healing; An Animal Model Study. *Bull Emerg. Trauma*. **2019,** 7, 366-372.
21. Anpo, M.; Kamat, P. Environmentally benign photocatalysts: Applications of Titanium oxide-based materials. **2010**.
22. Hamdan, S.; Pastar, I.; Drakulich, S.; Dikici, E.; Tomic-Canic, M.; Deo, S.; Daunert, S. Nanotechnology-Driven Therapeutic Interventions in Wound Healing: Potential Uses and Applications. *ACS. Central Science*. **2017**, 3, 163-175.
23. Balouiri M.; Sadiki M.; Ibnsouda S.K. Methods for in vitro evaluating antimicrobial activity: A review, *J. Pharm. Anal*. **2016**, 6, 71-79.

24. Appiah, T.; Boakye, Y.D.; Agyare, C. Antimicrobial activities and time-kill kinetics of extracts of selected ghanaian mushrooms. *Evid Based Complement Alternat Med.* **2017**, 4534350.
25. Stepanović, S.; Vuković, D.; Hola, V.; Di Bonaventura, G.; Djukić, S.; Cirković, I.; Ruzicka, F. Quantification of biofilm in microtiter plates: overview of testing conditions and practical recommendations for assessment of biofilm production by staphylococci. *APMIS.* **2007**, 115, 891-899.
26. Cruz, C. D.; Shah, S.; Tammela, P. Defining conditions for biofilm inhibition and eradication assays for gram-positive clinical reference strains. *BMC Microbiology.* **2018**, 18(1), 173.
27. Marini, L.; Rojas, M.A.; Sahrmann, P.; Aghazada, R.; Pilloni, A. Early wound healing score: a system to evaluate the early healing of periodontal soft tissue wounds. *J. Periodontal Implant. Sci.* **2018**, 48, 274-283.
28. Naghili, H.; Tajik, H.; Mardani, K.; Razavi Rouhani, S.M.; Ehsani, A.; Zare, P. Validation of drop plate technique for bacterial enumeration by parametric and nonparametric tests. *Vet. Res. Forum.* **2013**, 4, 179-183.
29. Sultana, J.; Molla, M.R.; Kamal, M.; Shahidullah, M.; Begum, F.; Bashar, M.A. Histological differences in wound healing in maxillofacial region in patients with or without risk factors. Bangladesh *J. Pathol.* **2009,** 24, 3-8.
30. Santos, T.S.; Santos, I.; Pereira-Filho, R.N.; Gomes, S.V.F.; Lima-Verde, I.B.; Marques, M.N.; Cardoso, J.C.; Severino, P.; Souto, E.B.; Albuquerque-Júnior, R.L.C. Histological evidence of wound healing improvement in rats treated with oral administration of hydroalcoholic extract of Vitis labrusca. *Curr. Issues Mol. Biol.* **2021,** 43, 335-352.
31. Zadrazilova, I.; Pospisilova, S.; Pauk, K.; Imramovsky, A.; Vinsova, J.; Cizek, A.; Jampilek, J. In vitro bactericidal activity of 4- and 5-chloro-2-hydroxy-N-[1-oxo-1-(phenylamino) alkan-2-yl benzamides against MRSA. *Biomed. Res. Int.* **2015,** 349534.
32. Joseph, E.; Singhvi, G. Chapter 4-Multifunctional nanocrystals for cancer therapy: a potential nanocarrier, In: Nanomaterials for drug delivery and therapy. William Andrew Publishing, **2019**, 91-116.
33. Ostolska, I.; Wiśniewska, M. Application of the zeta potential measurements to explanation of colloidal Cr(2)O(3) stability mechanism in the presence of the ionic polyamino acids. *Colloid Polym. Sci.* **2014**, 292, 2453-2464.
34. Godoy-Gallardo, M.; Eckhard, U.; Delgado, L.M.; de Roo Puente, Y.J.D.; Hoyos-Nogues, M.; Gil, F.J.; Perez, R.A. Antibacterial approaches in tissue engineering using metal ions and nanoparticles: From mechanisms to applications. *Bioact. Mater.* **2021**, 6, 4470-4490.
35. Breijyeh, Z.; Jubeh, B.; Karaman, R. Resistance of gram-egative bacteria to current antibacterial agents and approaches to resolve it. *Molecules.* **2020**, 25.
36. Shi, H.; Magaye, R.; Castranova, V.; Zhao, J. Titanium dioxide nanoparticles: a review of current toxicological data. *Part. Fibre. Toxicol.* **2013**, 10, 15.
37. Ruppé, É.; Woerther, P.L.; Barbier, F. Mechanisms of antimicrobial resistance in gram-negative bacilli. *Ann. Intensive Care.* **2015**, 5, 61.
38. Pulgarin, C.; Kiwi, J.; Nadtochenko, V. Mechanism of photocatalytic bacterial inactivation on TiO2 films involving cell-wall damage and lysis. Applied Catalysis B. *Environmental.* **2012**, 128, 179-183.
39. Di Pilato, V.; Ceccherini, F.; Sennati, S. F. D'Agostino, F. Arena, N. D'Atanasio, F. P. Di Giorgio, S. Tongiani, L. Pallecchi and G. M. Rossolini. In vitro time-kill kinetics of dalbavancin against Staphylococcus spp. biofilms over prolonged exposure times. *Diagn. Microbiol. Infect. Dis.* **2020**, 96(2), 114901.
40. Archer, N. K.; Mazaitis, M. J.; Costerton, J. W.; Leid, J. G.; Powers, M. E.; Shirtliff, M. E. Staphylococcus aureus biofilms: properties, regulation, and roles in human disease. *Virulence.* **2011**, 2(5), 445-459.
41. Carrouel, F.; Viennot, S.; Ottolenghi, L.; Gaillard, C.; Bourgeois, D. Nanoparticles as antimicrobial, anti-inflammatory, and remineralizing agents in oral care cosmetics: A review of the current situation. *Nanomaterials.* **2020**, 10(1), 140.
42. Xu, S.; Sun, T.; Xu, Q.; Duan, C.; Dai, Y.; Wang, L.; Song, Q. Preparation and antibiofilm properties of Zinc oxide/porous anodic alumina composite films. *Nanoscale Res. Lett.* **2018**, 13, 201.
43. Khatoon, Z.; McTiernan, C.D.; Suuronen, E.J.; Mah, T.-F.; Alarcon, E.I. Bacterial biofilm formation on implantable devices and approaches to its treatment and prevention. *Heliyon.* **2018**, 4.
44. Hou, Y.; Cai, K.; Li, J.; Chen, X.; Lai, M.; Hu, Y.; Luo, Z.; Ding, X.; Xu, D. Effects of Titanium nanoparticles on adhesion, migration, proliferation, and differentiation of mesenchymal stem cells. Int *J. Nanomedicine.* **2013**, 8, 3619-3630.
45. Chermprapai, S.; Ederveen, T. H. A.; Broere, F.; Broens, E. M.; Schlotter, Y. M.; van Schalkwijk, S.; Boekhorst, J.; van Hijum S. A. F. T.; Rutten, V. P. M. G. The bacterial and fungal microbiome of the skin of healthy dogs

and dogs with atopic dermatitis and the impact of topical antimicrobial therapy, an exploratory study. *Vet. Microbiol.* **2019**, 229, 90-99.

46. Mathew-Steiner, S. S.; Roy, S.; Sen, C. K. Collagen in wound healing. *Bioengineering (Basel).* **2021**, 8, 5.